54506 7

POPULAR SUMMARY
HJZ, August 16, 2001

Balance Mass Flux and Velocity Across the Equilibrium Line in Ice Drainage Systems of Greenland

H. Jay Zwally and Mario B. Giovinetto

Estimates of balance mass flux and the depth-averaged ice velocity through the cross-section aligned with the equilibrium line are produced for each of six drainage systems in Greenland. (The equilibrium line, which lies at approximately 1200 m elevation on the ice sheet, is the boundary between the area of net snow accumulation at higher elevations and the areas of net melting at lower elevations around the ice sheet.) Ice drainage divides and six major drainage systems are delineated using surface topography from ERS radar altimeter data. The net accumulation rate in the accumulation zone bounded by the equilibrium line is 399 Gt/yr and net ablation rate in the remaining area is 231 Gt/yr . (1 GigaTon of ice is 1090 km^3.) The mean balance mass flux and depth-averaged ice velocity at the cross-section aligned with the modeled equilibrium line are 0.1011 Gt km^{-2}/yr and 0.111 km/yr, respectively, with little variation in these values from system to system. The ratio of the ice mass above the equilibrium line to the rate of mass output implies an effective exchange time of approximately 6000 years for total mass exchange. The range of exchange times, from a low of 3 ka in the SE drainage system to 14 ka in the NE, suggests a rank as to which regions of the ice sheet may respond more rapidly to climate fluctuations.

Balance mass flux and ice velocity across the equilibrium line in drainage systems of Greenland

H. Jay Zwally
NASA Goddard Space Flight Center, Greenbelt, Maryland

Mario B. Giovinetto
Raytheon TSC - ITSS, Greenbelt, Maryland

Abstract. Estimates of balance mass flux and depth-averaged ice velocity through the cross section aligned with the equilibrium line are produced for each of six drainage systems in Greenland. The estimates are based on a model equilibrium line fitted to field data and on a revised distribution of surface mass balance for the conterminous ice sheet. Ice drainage divides and six major drainage systems are delineated using surface topography from ERS radar altimeter data. Ice thicknesses at the equilibrium line and throughout each drainage system are based on the latest compilation of airborne radar sounding data described elsewhere. The net accumulation rate in the area bounded by the equilibrium line is 399 Gt a^{-1}, and net ablation rate in the remaining area is 231 Gt a^{-1}. Excluding an east central coastal ridge reduces the net accumulation rate to 397 Gt a^{-1}, with a range from 42 to 121 Gt a^{-1} for the individual drainage systems. The mean balance mass flux and depth-averaged ice velocity at the cross-section aligned with the modeled equilibrium line are 0.1011 Gt km^{-2} a^{-1} and 0.111 km a^{-1}, respectively, with little variation in these values from system to system. In contrast, the mean mass discharge per unit length along the equilibrium line ranges from one half to double the overall mean rate of 0.0468 Gt km^{-1} a^{-1}. The ratio of the ice mass in the area bounded by the equilibrium line to the rate of mass output implies an effective exchange time of approximately 6 ka for total mass exchange. The range of exchange times, from a low of 3 ka in the SE drainage system to 14 ka in the NE, suggests a rank as to which regions of the ice sheet may respond more rapidly to climate fluctuations.

1. Introduction

Ice sheets interactions with the atmosphere, ocean, and Earth's crust are part of feedback processes that are important components in studies of global change [e.g., Warrick *and Oerlemans*, 1990; *Warrick et al.*, 1996]. Reliable modeling of ice sheet dynamics is essential to those studies. Description of boundary conditions of ice sheets at or near steady state, i.e., equilibrium between mass input and output rates or a net mass budget of zero, is critical for model development [e.g., *van der Veen and Whillans*, 1990; *Huybrechts and De Wolde*, 1999].

In this paper, estimates of balance mass flux (Gt km^{-2} a^{-1}) at cross sections aligned with the equilibrium line are derived for six major drainage systems in Greenland. Related quantities, the balance mass discharge per unit length across the equilibrium line (Gt km^{-1} a^{-1}) and the depth-averaged balance velocity (km a^{-1}) at the equilibrium line are estimated. The equilibrium line is chosen for analysis, because in effect, all the ice added in the accumulation zone above the equilibrium line of the ice sheet passes through the cross section at the equilibrium line. Although modified by transverse convergence or divergence, the balance mass discharge (of ice) per unit length tends to increase from high elevations to a maximum at the equilibrium and then decrease toward the margins of the ice sheet. Moreover, the ratios between the total ice mass for the area bounded by the equilibrium line and the balance mass output (Tt $(Gt\ a^{-1})^{-1}$ = ka) for the various drainage systems suggest which part or parts of the ice sheet would react more rapidly to climate fluctuations and changes in boundary conditions. For these purposes we compile new descriptions of the location of the

equilibrium line and revise a recent distribution surface balance. We also delineate drainage divides, estimate the area of the cross section aligned with the equilibrium line, and estimate the ice mass of each drainage system.

2. Equilibrium Line Location and Surface Balance

The location of the equilibrium line is variable from year to year and is regionally dependent on complex feedbacks discussed in preceding compilations [e.g., *Benson*, 1962; *Reeh*, 1985; *Weidick*, 1995]. It has been described on the basis of single elevation and latitude schemes applied to the whole ice sheet, typically with caveats on the differences between eastern and western flanks, as well as between north- and south-facing slopes [e.g., *Warrick and Oerlemans*, 1990; *Giovinetto and Zwally*, 1995]. Our new compilations of equilibrium line altitude (ELA) as a function of latitude, one each for eastern and western Greenland (Figure 1), are based on ELA data summarized in the preceding compilations [*Benson*, 1962; *Reeh*, 1985; *Weidick*, 1995] supplemented by additional reports [*Lister*, 1956; *Blatter and Ohmura*, 1991; *van de Wal et al.*, 1995]. First, we defined an "interpolated" equilibrium line using linear variations of the ELA between data sites. Second, we define a "model" equilibrium line, a function of latitude derived by second-order polynomial fits to the same field data:

$$\mathrm{ELA}e = -32759.680 + (1001.782 * L) - (7.331 * L^2): \quad R=0.998;\ R^2=0.997;\ \mathrm{RMS} = 50, \tag{1}$$

$$\mathrm{ELA}w = -23201.445 + (746.249 * L) - (5.640 * L2): \quad R=0.819;\ R^2=0.671;\ RMS = 298, \tag{2}$$

where ELA*e* and ELA*w* are the elevation (in meters) of the equilibrium line along the eastern and western regions, respectively, L is latitude (in degrees), R and R^2 are the coefficients of correlation and determination, respectively, and RMS is the root-mean-square residual (in meters). As expected, the RMS values are large, but are representative of the interannual variability observed in the field [e.g., *LaChapelle*, 1955; *Thomsen et al.*, 1988; *van de Wal et al.*, 1995]. Although higher-order polynomials produce slightly improved R values (but not the RMS values), the paucity of the data does not justify a more complex formulation.

Both the interpolated and the model equilibrium lines are an improvement over the single generalized relationship applied to both eastern and western regions in a preceding study (i.e., a linear variation from 300 m at 81°N to 1800 m at 62°N [*Giovinetto and Zwally*, 1995; *Zwally and Giovinetto*, 2000]). However, we consider the modeled line to be a better representation of the equilibrium by its averaging over interannual variability included in the field data. Although a single second-order polynomial model for both the eastern and the western regions (ELA*ew*, in meters):

$$\mathrm{ELA}ew = -21741.018 + (701.096 * L) - (5.292 * L^2): \quad R=0.862,\ R^2=0.743,\ \mathrm{RMS} = 264\ \mathrm{m}, \tag{3}$$

is more robust than a simple linear regression model (R=0.717, R^2=0.514, RMS = 347 m), the separate equations may better represent the east and west variations with latitude.

In this study we use the model equilibrium line to revise the distribution of surface balance in relatively narrow zones above and below the equilibrium line (Figure 2) and estimate the respective areas in the accumulation and ablation zones. The estimate of surface balance is based on 50 km grid values (Plate 1) obtained from a combination of three sources, each applied to particular zones defined by glacial facies [*Zwally*

Figure 1

Figure 2

Plate 1

and Giovinetto, 2000]. The surface balance values are obtained differently in three zones. For the zone above the intrapercolation line (dry snow plus upper percolation facies) the balance is derived from passive-microwave and surface temperature data using the model of *Zwally and Giovinetto* [1995]. The model was developed as a best fit to field data from sites in the area bounded by the dry snow line. For the zone between the intrapercolation and equilibrium lines, the balance is obtained by visual interpolation from the accumulation isopleths pattern of *Ohmura and Reeh* [1991] drawn on the basis of interpolation and extrapolation of field data. For the ablation zone below the equilibrium line, the balance is a function of surface elevation and latitude from the ablation nomogram of *Braithwaite* [1980], which is based on a parameterization of the rate of ablation and surface energy balance for the zone below the equilibrium line. Although the ablation model was developed for western Greenland, we use it for all of Greenland.

Surface balance values for grid point locations closest to either side of the equilibrium line are adjusted following the format of the rate change over distance, as described elsewhere for the area below the ELA [*van de Wal et al.*, 1995] and for the area above the ELA [*Zwally and Giovinetto*, 2000]. The 682 grid points that sample the area of the conterminous ice sheet are distributed over 49 grid lines and 126 grid squares form the perimeter. Surface balance values were adjusted for approximately one half of the 250 grid point locations that lie closest to either side of the equilibrium line.

The revised distribution of the accumulation and ablation rates and new estimates of surface balance are given in Table 1. The bulk accumulation and ablation rates are the rates integrated over the respective accumulation or ablation zones. The estimates of area and accumulation are based on the number of grid points sampling a particular area, and all estimates are weighted by the actual area of each grid square. The grid point locations in the 50 km grid database are determined on a polar stereographic projection with a standard line at 71°N. Each point location is centered on a grid square with a nominal area of 2500 km^2 which is adjusted for projection deformation. The actual area of a grid square (AGS) (in square kilometers) is obtained using

$$AGS = [-0.132 + (0.026 * L) - (1.441^{-4} * L^2)] 2500. \quad (4)$$

The changes from the revisions are summarized as follows:

1. The area of the accumulation zone decreases from 91 % to 88 % of the total area of the conterminous ice sheet (N = 682, 1.6913 x 10^6 km^2), i.e., from N = 620 to N = 597 or from 1.5415 x 10^6 km^2 to 1.4840 x 10^6 km^2. The mean rate of accumulation for the area bounded by the equilibrium line increases by 2 % (from 263 to 267 kg m^{-2} a^{-1}), and due to the decrease in area, the estimate of bulk accumulation decreases by 1 % (from 405 to 399 Gt a^{-1}).

2. The area of the ablation zone increases from 9 % to 12 % of the total area of the conterminous ice sheet, i.e., from N = 62 to N = 85, or from 0.1497 x 10^6 km^2 to 0.2073 x 10^6 km^2). The mean rate of ablation for the area decreases by 14 % (from -1259 to -1086 kg m^{-2} a^{-1}), and due to the increase in area, the bulk ablation estimate increases by 23 % (from -188 to -231 Gt a^{-1}).

3. Overall, for the conterminous ice sheet (N = 682, 1.6913 x 10^6 km^2), the estimate of surface balance decreases by 23 % (from 128 to 99 kg m^{-2} a^{-1}), and the estimate of bulk accumulation decreases by 22 % (from 216 to 168 Gt a^{-1}). The discrepancy in the percent value is due to using round-off numbers in the integration.

Using equations (1) and (2) for ELA as a function of latitude, the location of both the modeled and the interpolated

Table 1

Plate 2

equilibrium lines (Plate 2) are traced on the ice sheet topographic sheets with contour increments of 100 m produced from the ERS-1 database [*Zwally and Brenner*, 2001] at a scale of approximately 1 : 2 x 10^6. In regions such as the NE and SE the location of the lines are practically coincident. In others, such as the SW at 66°N, the interpolated line is approximately 300 m higher than the model line, and the horizontal difference is approximately 40 km. The variations in location of the lines determine the first accumulation isopleth that can be drawn with confidence along the periphery of particular sectors. This and other limitations are imposed by the small scale of the Figure 2 map and by the coarse 50 km database, which make it impossible to draw isopleths at regular increments everywhere. We also make small revisions to the isopleths pattern drawn in the interior (but no changes in grid point values) relative to that shown in a preceding study [*Zwally and Giovinetto*, 2000].

3. Drainage Divides and Systems

The drainage divides (Plate 3) are delineated on the basis of ERS radar altimeter data analyzed to yield surface maximum slope gradient and direction at a 5 km grid resolution [*Zwally and Brenner*, 2001]. The six major drainage systems selected each include a minimum of three subbasins, as shown by a flow line scheme based on a 20 km grid interpolated from the 5 km ERS-1 grid (Figure 3) (W. L. Wang, personal communication, 2000). However, considerably more data on accumulation, and particularly on ice thickness as well as bed topography, would be required to produce the same type of estimates at subbasin scale.

Plate 3

Figure 3

The drainage divide along the main N-S ridge is joined by divides that originate in distinct localities near the periphery of the conterminous ice sheet. The primary criterion for the selection of the localities is that the divides split the flanks of the ice sheet in entities of relatively homogeneous surface-slope orientation, as this will determine other important characteristics such as orographic influence on precipitation. Among secondary criteria, we considered coherence relative to distance to open ocean, as this has influence on the rate of accumulation [e.g., *Zwally and Giovinetto*, 1997] and area size. We list below the points at or near the ice terminus of each drainage divide, because unlike divide-intersection points in the interior these points are difficult to identify on topographic maps: 1 and 2: 80.70°N, 27.0°W, thence NE to the ice terminus; 2 and 3: 75.00°N, 23.0°W, thence ESE to the ice terminus; 3 and 4: 66.70°N, 35.9°W, thence SE to the ice terminus; 4 and 5: 61.58°N, 47.7°W; 5 and 6: 71.96°N, 52.4°W, thence SW to the ice terminus; 6 and 1: 76.21°N, 68.5°W, thence WSW to the ice terminus. The area of each system is estimated on the basis of the number of grid points that lie within the boundaries set by the divides, adjusted as per equation (4).

System 3 is listed twice (Table 2) because the relatively small ice ridge extending ENE from approximately 69.68°N, 29.8°W distorts the comparison with the other systems. Its exclusion is implicit throughout the discussions that follow, unless stated otherwise. We refer herein to system "3 modified" as 3m and to any summary statistics for the whole ice that includes 3m as systems 1-6m. Nevertheless, we list the statistics for both system 3 and systems 1-6 for completeness. In the same context we present details of the estimates of accumulation and ablation produced from the application of the model equilibrium line for each system to facilitate future comparison with results of mass budget studies.

Table 2

Relative to the total area of the conterminous ice sheet (systems 1-6: 1.6913 x 10^6 km^2), the whole area of each system, i.e., the sum of the areas of net accumulation and net ablation, range between 10 % and 25 % (from 0.1683 x 10^6 km^2 in system 4 to 0.4312 x 10^6 km^2 in system 5, respectively). Relative to the total area bounded by the model equilibrium line (systems 1-6m: 1.4767 x 10^6 km^2), the range reduced slightly to between 9 % and 24 %, all systems ranked in the same order (from 0.1310 x 10^6 km^2 in system 4 to 0.3516 x 10^6 km^2 in system 5, respectively).

The accumulation values for grid squares (Plate 1) are used to obtain mean values in kg m^{-2} a^{-1}, or integrated to obtain bulk values in Gt a^{-1}, for the whole area of each system. It should be noted that the area of the ice sheet (systems 1-6) lying above ELA is estimated to be 88 % of the total area and that this statistic does not change when the area above ELA for systems 1-6m is considered. However, it shows a relatively large range between 78 % in system 4 and 96 % in system 1. The size of the range is important because different "placements" of the equilibrium line are generally the principal source for the difference between any two surface balance estimates reported in the literature, regardless of the total area assigned to the ice sheet [*Zwally and Giovinetto*, 2000]. Closely related to this statistic, the ratio between the areas of net ablation and net accumulation also emphasizes the physiographic differences between systems; whereas the ratio for systems 1-6m is 0.14, the range for particular systems range between 0.04 for system 1 and 0.28 for system 4.

An interesting characteristic of our results is the wide variation in the mean accumulation in the area above the equilibrium line among the drainage systems, ranging from 134 to 509 kg m^{-2} a^{-1} for systems 2 and 4, respectively. The variation is from one half to twice the mean for all systems (267 kg m^{-2} a^{-1}). The bulk accumulations for each drainage system range from 42 Gt a^{-1} for system 2 to 121 Gt a^{-1} for system 5. The total bulk accumulation for systems 1-6m is 397 Gt a^{-1}.

4. Equilibrium Line Cross Section and Balance Mass Output Estimates

Ice thickness determinations are needed to estimate the mean ice depth at the output cross section defined by the equilibrium line and for an area bounded by it. All ice thickness determinations are produced from the 5 km grid PARCA/TUD database (J.L. Bamber, personal communication, 2000) [*Bamber et al.*, this issue]. The mean ice depth at the output cross section is obtained directly from the 5 km grid database. The mean ice thickness for the area bounded by the equilibrium line is estimated in two steps. The first step produces an ice thickness value for each grid point location in our 50 km grid by bilinear interpolation [*Research Systems Inc.*, 1999] from the 5 km grid database. This value applies to the grid point location and is not the mean thickness averaged over the 2500 km^2 area of each grid square. The second step produces the mean ice thickness and total ice mass values for each drainage system from the values compiled in our 50 km grid database. This coarse sampling method is internally consistent with the compilation approach used for many other variables in the 50 km grid database used in this and preceding studies.

The length of the equilibrium line, as well as the mean ice thickness and cross-sectional area at the line, are listed in Table 3. The range of cross-sectional areas is large, from 459 km^2 in system 1 to 1022 km^2 in system 5. The total cross-sectional area for systems 1-6m is 3773 km^2.

Table 3

The balance mass fluxes through the equilibrium line are the ratio of bulk net mass accumulation in the accumulation zones to the area of the cross section at the equilibrium line. In contrast to the factor of 3 range in bulk accumulations, the balance fluxes only range from 0.0907 Gt km^{-2} a^{-1} in system 3m to 0.1181 in system 5, which is less than a 20% variation about the mean of 0.1011 Gt km^{-2} a^{-1}. The depth-averaged balance velocities at the equilibrium line also have a small variation, ranging from 0.100 km a^{-1} in system 3m to 0.130 km a^{-1} in system 5, about a mean of 0.111 km a^{-1} for all systems 1-6m.

A simplified characterization of the balance mass flux, which is independent of errors in the estimate of mean ice thickness at the output cross section, is the mass flow per unit length of the equilibrium line. Relative to a weighted mean of 0.0468 Gt km^{-1} a^{-1} for all systems 1-6m, the values for the separate drainage systems vary from 0.0208 Gt km^{-1} a^{-1} for system 1 to 0.0878 Gt km^{-1} a^{-1} for system 5.

The ratio of total ice mass above the equilibrium line to the balance mass output (Tt (Gt a^{-1})$^{-1}$ = ka) in each system provides a basis to infer the relative response time on the drainage systems to climate fluctuations. The effective exchange times, expressed as the number of millennia necessary to attain 100% equivalent throughput, ranges from a low of 3 ka in the southeast system 4 to a high of 14 ka in the northeast system 2 (Table 3). This range in times is from approximately one half to double the 6 ka value for the whole ice sheet. The estimates of mean ice thickness and ice mass for each drainage system are also listed in Table 3.

5. Estimates of Errors

The overall combined error that would apply to mass output estimates, such as flux, discharge per unit length of periphery, and depth-averaged velocity, includes errors on the estimates of area, accumulation, and ice thickness, each of which is a combined error term. All three of these parameters are also dependent on the errors pertaining to determinations of location and length of the equilibrium line. Some of the errors are relatively large. Moreover, the balance mass output estimates are for ice entities of large area and volume with long lapses between variations of mass input and corresponding variations of mass output.

The combined error terms for some of the estimates are readily assessed (e.g., terms introduced by coarse grid sampling affecting area and accumulation estimates). Other terms, however, would require detailed elaboration beyond the scope of this study. Among these are terms pertaining to the location and length of the equilibrium line, which could be assessed using RMS values given for equations (1) through (3), converting elevation change to distance over slope gradients, and terms pertaining to referenced ice thickness databases. Below, we assess some of the error terms and, for brevity, only as they apply to the whole area bounded by the equilibrium line rather than particular systems.

Coarse grid sampling introduces two terms in the combined error. One is in the estimate of area, assessed at one-fourth the area of each outer grid square. The area of systems 1-6 bounded by the equilibrium line (1.4840 x 10^6 km^2) is covered by 48 grid lines. There are 125 outer grid points and the error estimate is ± 0.0781 x 10^6 km^2 or ± 5 %. At a mean accumulation rate of 267 kg m^{-2} a^{-1} the error in area contributes ± 21 Gt a^{-1} to the combined error. The other term is an error of approximately ± 6 % relative to the accumulation estimate that could be obtained by detailed area integration of the accumulation rate as shown on isopleth maps [e.g., *Giovinetto and Zwally*, 2000]. At the mean

accumulation rate, this implies an error of ± 16 kg m^{-2} a^{-1} which contributes ± 24 Gt a^{-1} to the combined error.

The error in the estimate of accumulation is ± 42 kg m^{-2} a^{-1} applicable to the mean rate of 267 kg m^{-2} a^{-1} for the N = 597 data set. The relatively large error of ± 16 % contributes ± 62 Gt a^{-1} to the combined error. It is the area-weighted mean of two terms, one each for the grid point locations sampling the zones of dry and upper percolation facies (N = 442), and of lower percolation, wetted, and superimposed ice facies (N = 155). The relative error for the N = 442 data set has been assessed at ± 12 % of the mean rate [*Zwally and Giovinetto*, 1995], or ± 29 kg m^{-2} a^{-1} based on a mean rate of 241 kg m^{-2} a^{-1}. The relative error for the N = 155 data set is assumed to be greater by at least a factor of 2 (± 24 %), or ± 82 kg m^{-2} a^{-1} based on a mean rate of 341 kg m^{-2} a^{-1}. The assumption attempts to assimilate the composite error inherent to the source compilation and to the procedure we use to obtain the values for the N = 155 data set. As stated in a preceding section, the values are obtained by visual interpolation from the isopleths pattern of *Ohmura and Reeh* [1991]. The isopleths location are themselves subject to a composite error that includes the error in the determination of the rate at each field data site, the error due to spatial (areal) and temporal variabilities of accumulation because most of the data are unevenly distributed in space and time, and the error of interpolation and extrapolation to draw the isopleths pattern. Furthermore, approximately one half of the accumulation values for the125 grid point locations that lie closest to the equilibrium line are reduced to reach a value of zero at the line; this modification introduces an error of unknown value that nonetheless must be large.

The variation of each balance mass output estimate listed in this study is assumed to be in phase with any variation of mass input, lagging at least from several decades to a few centuries. The annual variability of accumulation has been estimated on the basis of relatively long series determined from core studies (± 25 kg m^{-2} a^{-1} [*van der Veen and Bolzan*, 1999]) which, if applied to the area bounded by the equilibrium line suggests a variability of ± 37 Gt a^{-1} and a standard error of the mean of the order of ± 1 Gt a^{-1} (possibly reaching a value of ± 5 Gt a^{-1}). The annual variability estimated from a 10 year net water vapor transport series produced by atmospheric numerical analyses (± 16 % as it can be deduced from a survey of the literature [*Calanca and Ohmura*, 1994; *Chen et al.*, 1997; *Bromwich et al.*, 1998]) suggests a variability for the area bounded by the equilibrium line of ± 64 Gt a^{-1} and a standard error of the mean of ± 20 Gt a^{-1}. The second and largest of the two temporal variability assessments, differences in approach withstanding, would contribute a term to the combined error of ± 5 %.

In summary, the combined error in estimates of mass output (the sum of the "standard" errors in the estimate of area (± 5 %), grid sampling approach (± 6 %), accumulation (± 16 %), and long-term temporal variability (± 5 %)) is ± 18 % or ± 73 Gt a^{-1}. In the context of balance flux, discharge and depth-averaged velocity findings of this study, ± 18 % should be considered a minimum error, as we have not made assessments of the terms corresponding to errors in the location of the equilibrium line, and of estimates of its length and ice thickness at the output cross section defined by it. Also excluded from the discussion is the error in the estimate of ice thickness for the area bounded by the equilibrium line, affecting only the estimate of time required for total exchange of mass.

6. Discussion and Conclusions

Important aspects of global change studies, in general, and of glaciological research, in particular, aim at reliable estimates of the mass budget of drainage systems and subbasins. Our purpose is to estimate the balance ice flux at the cross section aligned with the equilibrium line and infer which parts of the ice sheet may respond more rapidly to climate fluctuations and changes in boundary conditions. The total mass exchange rate information, expressed in millennia, suggests that southeastern Greenland (system 4, 2.7 ka) should react more rapidly to climatic fluctuations than northern Greenland (systems 1 and 2, 8.5 and 14.1 ka, respectively).

On the basis of additional field reports on the ELA, a previous linear decrease of ELA with latitude is replaced by a model equilibrium lines from a second-order polynomial fit to the data, one each for eastern and western Greenland. Another line that is linearly interpolated between the field data is also used for comparison. All four descriptions are sensitive to the greater accumulation rates southward of approximately 65°N, which together with other undetermined phenomena, depress the ELA. As an assessment of the effect that changes in the location of the equilibrium line introduce on surface balance estimates, we evaluated the balance for both lines. The model equilibrium line splits the area of the conterminous ice sheet into 88 % above and 12 % below the ELA. The interpolated equilibrium line splits the area into 89 % above and 11 % below the ELA. The difference in location of the line alters the distance between the line and the closest grid point locations on either side, thus introducing a large adjustment in the accumulation and ablation values due to the steep gradient of the balance rate. The estimates of net accumulation and net ablation obtained from application of the interpolated line are 399 and 231 Gt a^{-1}, respectively, and those obtained from the application of the model line are 402 and 200 Gt a^{-1}, respectively. The net surface balance estimates (168 Gt a^{-1} for the model line and 202 Gt a^{-1} for the interpolated line) indicate that differences of ± 20 % can be introduced depending on the criteria used to interpret the same ELA field data. To the extent that this difference is related to interannual variability of the ELA captured in the field data, it gives an indication of the large interannual variability in the net surface balance.

Our net surface balance estimate of 168 Gt a^{-1} is the smallest reported in the last two decades (Table 4) and practically identical in value to that reported by *Ohmura et al.* [1999]. However, only one other estimate (for the "inner equilibrium line" from *Radok et al.* [1982]) can be compared directly with ours, because of the common use of net accumulation and net ablation for the areas on either side of an "inner" equilibrium line. As previously discussed [*Zwally and Giovinetto*, 2000], the net surface balance for the inner equilibrium line from *Radok et al.* [1982] is larger by a factor of approximately 2. Direct comparison with all other estimates of surface mass balance, including that of *Ohmura et al.* [1999] is not possible because they are based on the difference between gross accumulation and gross ablation (at the surface) over the whole area of the ice sheet (generally including the area of outlying ice caps). Nevertheless, the difference between our estimate and those reported in three studies [*Weidick*, 1984; *van de Wal*, 1996; *Ohmura et al.*, 1999] is relatively small (i.e., between 1 and 55 Gt a^{-1}). The difference with the results reported in four other studies [*Reeh*, 1985; *Huybrechts et al.*, 1991; *Reeh et al.*, 1999; *Janssens and Huybrechts*, 2000] is relatively large (i.e., between 93 and 150 Gt a^{-1}). As expected, the difference between the various surface balance estimates is largely introduced by differences in the assessment of ablation. The

mean of the seven estimates of gross ablation cited above is 277 Gt a^{-1} with a standard deviation of 56 Gt a^{-1} or 20 %, whereas the same statistics for the corresponding gross accumulation estimates is 524 ± 23 Gt a^{-1} or ± 5 % and show practically no change (526 ± 21 Gt a^{-1} or ± 4 %) if three other estimates of gross accumulation are included [*Ohmura and Reeh*, 1991; *Robasky and Bromwich*, 1994] (F. Jung-Rothenhäusler et al., unpublished data, 2000). For these comparisons we excluded the one produced as a heuristic benchmark based on an "outer" equilibrium line [*Radok et al.*, 1982] and our preceding studies [*Giovinetto and Zwally*, 1995; *Zwally and Giovinetto*, 2000], which used a similar methodology.

The split of the whole area of systems 1-6 between zones of accumulation and ablation (1.4840 x 10^6 km^2 and 0.2073 x 10^6 km^2, respectively) is modified for the purposes of this study, excluding a relatively small coastal ridge area in system 3 (it becomes 3m), reducing the respective areas of systems 1-6m to 1.4767 x 10^6 km^2 and 0.1999 x 10^6 km^2. The modification does not change the area split of 88 % and 12 % for the areas of accumulation and ablation, respectively, although the area split varies between 78 % and 22 % for system 5 to 96 % and 4 % for system 1.

Our depth-averaged balance velocity estimates show general agreement with balance velocity fields described in other studies in which they are compared with those derived using radar interferometry methods. For example, there is general agreement with the results reported by *Joughin et al.* [1997], *Rignot et al.* [1995], and *Bamber et al.* [2000]. However, our mean estimates for drainage systems are generally not suitable for a detailed comparison with the fine-grid resolution analysis used in radar interferometry. Although it is probable that significant differences in the estimates of net accumulation at the surface would be found, accumulation comparisons are not practical because the other papers concentrate on the interferometry analyses rather than the particular accumulation databases used.

Comparison of our balance depth-average estimates are in close agreement (in the order of ±10 m a^{-1}) with the velocities determined by *Thomas et al.* [1998] for cross sections aligned approximately with the 2000 m surface elevation contour and which serve as discharge gates for an area including most of the area of system 6 as well as the northern one-third area of system 5. Moreover, in the northern part of system 5, at a latitude of 69.5°N and an elevation of 1250 m, surface motion measurements in 1967-1991 show a midrange value of 123 m a^{-1} [*Salbach*, 1995]. Our estimate for the system 5 indicates a mean of 130 m a^{-1}.

Further study of subbasins within the six defined drainage systems should show some significant departures from the calculated means. In system 2, for example, the ice stream bifurcates at approximately 77.0°N, 30.5°W, discharging farther downstream through two "gates", which at the cross section aligned with the equilibrium line are centered at approximately 77.6 °N, 24.5 °W, and 78.6 °N, 23.2 °W. The combined width of the gates is approximately 170 km and their mean ice thickness is approximately 0.5 km. The subbasin approximately delineated in Plate 3 is sampled by 59 grid points in the 50 km grid, giving an area of 0.15 x 10^6 km^2, a mean accumulation of 135 kg m^{-2} a^{-1}, and bulk accumulation of 20 Gt a^{-1}. The flux through the 85 km^2 output section is 0.24 Gt km^{-2} a^{-1}, with a discharge rate of 0.12 Gt km^{-1} a^{-1} and a depth-averaged velocity of 0.26 km a^{-1}. These output rates are approximately double those for the total system 2, even though the subbasin area and bulk accumulation are approximately one half the totals for the system.

Acknowledgments. The authors acknowledge the contributions of Matt Beckley in the compilation and analyses of databases and graphics, Wei Li Wang in producing the flowline map, and three anonymous reviewers for their comments and suggestions.

References

Ambach, W., Ansteigder CO2 - Konzentration in der Atmosphäre und Klimaanderung: Mögliche auswirkungen auf den grönlandischem Eisschild. *Wetter Leben, 32*, 135-142, 1982.

Bamber, J. L., R. J. Hardy, and I. Joughin, An analysis of balance velocities over the Greenland ice sheet and comparison with synthetic aperture radar interferometry. *J. Glaciol., 46*(152), 67-74, 2000.

Bamber, J. L., R. Layberry, and S. Gogineni, A new ice thickness and bed data set for the Greenland ice sheet, 1, Measurement, data reduction, and errors, *J. Geophys. Res.*, this issue.

Benson, C. S., Stratigraphic studies in the snow and firn of the Greenland ice sheet, Cold Reg. Res. and Eng. Lab., Hanover, New Hampshire, *Res. Rep. 70*, 1962.

Benson, C. S., Glacier facies: With special reference to Greenland, Geol. Surv. of Greenl., *Open File Ser. 94/13*, pp. 11-14, Copenhagen, Denmark, 1994.

Blatter, H., and A. Ohmura, ETH Greenland Expedition, 1, Project description, *Prog. Rep. 1*, pp. 9-16, Dep. of Geogr., Swiss Fed. Inst. of Technol., Zurich, Switzerland, 1991.

Braithwaite, R. J., Regional modelling of ablation in West Greenland, *Tech. Rep. 98*, Geol. Surv. of Greenl., Copenhagen, Denmark, 1980.

Bromwich, D. H., R. I. Cullather, W.-S. Chen, and B. M. Csatho, Evaluation of recent precipitation studies of the Greenland ice sheet, *J. Geophys. Res., 103*, 26,007 – 26,024, 1998.

Calanca, P., and A. Ohmura, Atmospheric moisture flux convergence and accumulation on the Greenland Ice Sheet, in *Snow and Ice Covers, Interactions With the Atmosphere and Ecosystems*, edited by H. G. Jones, T. D. Davis, A. Ohmura, and E. M. Morris, Int. Assoc. of Sci. Hydrol., *223*, 77-84, 1994.

Chen, Q.-S., D. H. Bromwich, and L. Bai, Precipitation over Greenland retrieved by a dynamic method and its relation to cyclonic activity, *J. Clim., 10*, 839-870, 1997.

Giovinetto, M.B., and H.J. Zwally, An assessment of the mass budgets of Antarctica and Greenland using accumulation derived from remotely sensed data on areas of dry snow, *Z. Gletscherk. Glazialgeol., 31*, 25-37, 1995.

Giovinetto, M.B., and H.J. Zwally, Spatial distribution of net surface accumulation on the Antarctic ice sheet, *Ann. Glaciol., 31*, 171-178, 2000.

Huybrechts, P., and J. de Wolde, The dynamic response of the Greenland and Antarctic ice sheets to multiple-century climatic warming, *J. Clim., 12*(8), 2169-2188, 1999.

Huybrechts, P., A. Letreguilly, and N. Reeh, The Greenland ice sheet and greenhouse warming. *Global Planet. Change, 3*(4), 399-412, 1991.

Janssens, I., and P. Huybrechts, The treatment of meltwater retention in mass-balance parameterisations of the Greenland ice sheet, *Ann. Glaciol., 3*, 133-140, 2000.

Joughin, I. R., M. A. Fahnestock, S. Ekholm, and R. Kwok, Balance velocities of the Greenland ice sheet, *Geophys. Res. Lett., 24*(23), 3045-3048, 1997.

LaChapelle, E., Ablation studies in the Mint Julep area, southwest Greenland, in *Project Mint Julep*, part 2, *Spec. Sci. Rep., Publ. A-104A*, U.S. Arct., Desert, Tropic Inf. Cent., Natick, Massachusetts, 1955.

Lister, H., British North Greenland Expedition, 1952-4: Scientific results, VI. Glacier regime in north-east Greenland, *Geogr. J., 122*(Part 2), 230-237, 1956.

Ohmura, A., and N. Reeh, New precipitation and accumulation maps for Greenland, *J. Glaciol., 37*(125), 140-148, 1991.

Ohmura, A., P. Calanca, M. Wild, and M. Anklin, Precipitation, accumulation and mass balance of the Greenland ice sheet. *Z. Gletscherk. Glazialgeol., 31*(1), 1-20, 1999.

Radok, U., R. G. Barry, D. Jenssen, R. A. Kenn, G. N. Kiladis, and B. McInnes, Climatic and physical characteristics of the Greenland Ice Sheet, parts I and II, Coop. Inst. for Res. in Environ. Sci., University of Colo., Boulder, Colorado, 1982.

Reeh, N., Greenland ice-sheet mass balance and sea-level change. in Glaciers, Ice Sheets, and Sea Level: Effect of a CO_2-Induced Climatic Change, *Rep. DOE/ER/60235-1*, pp. 155-171, U.S. Dep. of Energy, Washington D. C. 1985.

Reeh, N., C. Mayer, H. Miller, H. Hojmark Thomsen, and A. Weidick, Present and past climate control on fjord glaciations in Greenland: Implications for IRD-deposition in the sea, *Geophys. Res. Lett.*, *26*(8), 1039-1042, 1999.

Research Systems Inc., IDL Reference Guide A-M, IDL Version 5.3, September 1999 ed., Research Systems, Inc., Boulder, Colorado, 1999.

Rignot, E., K. C. Jezek, and H. G. Sohn, Ice flow dynamics of the Greenland ice sheet from SAR interferometry, *Geophys. Res. Lett.*, *22*(5), 575-578, 1995.

Robasky, F. M., and D. H. Bromwich, Greenland precipitation estimates from the atmospheric moisture budget, *Geophys. Res. Lett.*, *21*(23), 2485-2498, 1994.

Salbach, H., Determination of the dynamical behaviour of the Greenland ice sheet, *Z. Gletscherk. Glazialgeol.*, *31*(1), 65-71, 1995.

Thomas, R. H., B. M. Csatho, S. Gogineni, K. J. Jezek, and K. Kuivinen, Thicknening of the western part of the Greenland ice sheet, *J. Glaciol.*, *44*(128), 653-658, 1998.

Thomsen, H. H., L. Thorning, and R. J. Braithwaite, Glacier-hydrological conditions on the Inland Ice north-east of Jakobshavn/Ilusissat, West Greenland, *Rep. 138*, Grönl. Geol. Undersogelse, Copenhagen, Denmark, 1988.

van de Wal, R. S. W., Mass balance modelling of the Greenland ice sheet: A comparison of an energy balance and a degree-day model. *Ann. Glaciol.*, *23*, 36-45, 1996.

van de Wal, R. S. W., et al., Mass balance measurements in the Sondre Stromfjord area in the period 1990-1994. *Z. Gletscherk. Glazialgeol.*, *31*(1), 57-63, 1995.

van der Veen, C. J., and J. F. Bolzan, Flow laws for glacier ice: Comparison of numerical predictions and field measurements, *J. Glaciol.*, *36*(124), 324-339, 1999.

van der Veen, C. J., and I. M. Whillans, Interannual variability in net accumulation on the Greenland ice sheet: Observations and implications for mass balance measurements, *J. Geophys. Res.*, *104*, 2009-2014, 1990.

Warrick, R. A., and J. Oerlemans, Sea level rise, in *Climate Change, The IPCC Scientific Assessment*, edited by J. T. Houghton, G. J. Jenkins, J. J. Ephraums, pp. 260-281, Cambridge Univ. Press, New York, 1990.

Warrick, R. A., C. Le Provost, M. F. Meier, J. Oerlemans, P. L. Woodworth, Changes in sea level, in *Climate Change 1995, The Science of Climate Change*, edited by J. T. Houghton, L. G. Meira Filho, B. A. Callander, N. Harrris, A. Klattenberg, and K. Maskell, pp. 359-405, Cambridge Univ. Press, New York, 1996.

Weidick, A., Review of glacier changes in West Greenland. *Z. Gletscherk. Glazialgeol.*, *21*, 301-309, 1984.

Weidick, A., *Greenland. U.S. Geol. Surv. Prof. Pap. 1386-C, C1-C93*, Washington, D. C., 1995.

Zwally, J. H., and A. C. Brenner, The role of satellite radar altimetry in the study of ice sheet dynamics and mass balance, in *Satellite Altimetry and Earth Sciences*, edited by Lee-Leung Fu, pp. 351-369, Academic Press, San Diego, California, 2001.

Zwally, J. H., and M. B. Giovinetto, Accumulation in Antarctica and Greenland derived from passive microwave data: A comparison with contoured compilations, *Ann. Glaciol.*, *21*, 123-130, 1995.

Zwally, J. H., and M. B. Giovinetto, Annual sea level variability induced by changes in sea ice extent and accumulation on the ice sheets: An estimate based on remotely sensed data, in *Geophysical Evidence of Past and Present Climate Change, Surv. Geophys.*, *18*, 327-340, 1997.

Zwally, J. H., and M. B. Giovinetto, Spatial distribution of surface mass balance on Greenland, *Ann. Glaciol.*, *31*, 126-132, 2000.

H. J. Zwally, NASA Goddard Space Flight Center, Code 971, Greenbelt, MD 20771. (jay.zwally@gsfc.nasa.gov)

M. B. Giovinetto, Raytheon TSC - ITSS, NASA Goddard Space Flight Center, Code 971, Greenbelt, MD 20771. (mario.giovinetto@gsfc.nasa.gov)

(Received August 15, 2000; revised January 8, 2001; accepted January 23, 2001)

Paper number 2001JD900120.

Tables (pages 15 - 18)

Figure captions

Figure 1. Elevation of the equilibrium line in eastern and western Greenland relative to latitude. The "interpolated" equilibrium line is shown with solid lines (circles indicate the location of field data sites). The "model" equilibrium line is shown with diamonds (based on the same field data, each described by a second-order polynomial). The single generalized relationship applied to both eastern and western regions in earlier studies [*Giovinetto and Zwally*, 1995; *Zwally and Giovinetto*, 2000] is shown with dashed lines for comparison.

Figure 1. Elevation of the equilibrium line in eastern and western Greenland relative to latitude. The "interpolated" equilibrium line is shown with solid lines (circles indicate the location of field data sites). The "model" equilibrium line is shown with diamonds (based on the same field data, each described by a second-order polynomial). The single generalized relationship applied to both eastern and western regions in earlier studies [Giovinetto and Zwally, 1995; Zwally and Giovinetto, 2000] is shown with dashed lines for comparison.

Figure 2. Schematic distribution of accumulation as described in the 50 km grid relative to diagenetic facies and accumulation zones (modified after *Zwally and Giovinetto* [2000]). The number of grid point locations in the net ablation zone (N = 79) is determined by the location of the model equilibrium line. Grid point accumulation values are obtained from three sources (top bar); values for grid point locations closest and on either side of the equilibrium line are modified following criteria cited in the text

Figure 2. Schematic distribution of accumulation as described in the 50 km grid relative to diagenetic facies and accumulation zones (modified after *Zwally and Giovinetto* [2000]). The number of grid point locations in the net ablation zone (N = 79) is determined by the location of the model equilibrium line. Grid point accumulation values are obtained from three sources (top bar); values for grid point locations closest and on either side of the equilibrium line are modified following criteria cited in the text

Plate 1. Distribution of net accumulation at the surface on the conterminous ice sheet based on the 50 km grid database and model equilibrium line (modified after *Zwally and Giovinetto* [2000]).

Plate 1. Distribution of net accumulation at the surface on the conterminous ice sheet based on the 50 km grid database and model equilibrium line (modified after *Zwally and Giovinetto* [2000]).

Plate 2. Contoured distribution of net mass accumulation at the surface, showing the simplified outer coastline, ice terminus (dashed red line where it is not coincident with the coastline), interpolated and model equilibrium lines (solid orange and solid green, respectively), and accumulation isopleths labeled in kg m^{-2} a^{-1} (x 100); rate increments between isopleths are not regular because of map scale limitations (modified after *Zwally and Giovinetto* [2000]).

Plate 2. Contoured distribution of net mass accumulation at the surface, showing the simplified outer coastline, ice terminus (dashed red line where it is not coincident with the coastline), interpolated and model equilibrium lines (solid orange and solid green, respectively), and accumulation isopleths labeled in kg m^{-2} a^{-1} (x 100); rate increments between isopleths are not regular because of map scale limitations (modified after *Zwally and Giovinetto* [2000]).

Plate 3. Drainage divides and number designation of drainage systems, showing the simplified outer coastline, ice terminus (dashed red line where it is not coincident with the coastline), interpolated and model equilibrium line (solid orange and solid green, respectively), and the approximate delineation of the subbasin corresponding to the main ice stream in system 2 (long dashed lines).

Plate 3. Drainage divides and number designation of drainage systems, showing the simplified outer coastline, ice terminus (dashed red line where it is not coincident with the coastline), interpolated and model equilibrium line (solid orange and solid green, respectively), and the approximate delineation of the subbasin corresponding to the main ice stream in system 2 (long dashed lines).

Figure 3. Flow lines based on a 20 km grid calculated by W.L. Wang (personal communication, 2000) produced by interpolation from the 5 km grid database derived from ERS-1 radar altimeter data [*Zwally and Brenner*, 2001].

Figure 3. Flow lines based on a 20 km grid calculated by W.L. Wang (personal communication, 2000) produced by interpolation from the 5 km grid database derived from ERS-1 radar altimeter data [*Zwally and Brenner*, 2001].

Running Heads

ZWALLY AND GIOVINETTO: MASS FLUX IN DRAINAGE SYSTEMS OF GREENLAND

ZWALLY AND GIOVINETTO: MASS FLUX IN DRAINAGE SYSTEMS OF GREENLAND
ZWALLY AND GIOVINETTO: MASS FLUX IN DRAINAGE SYSTEMS OF GREENLAND
ZWALLY AND GIOVINETTO: MASS FLUX IN DRAINAGE SYSTEMS OF GREENLAND
ZWALLY AND GIOVINETTO: MASS FLUX IN DRAINAGE SYSTEMS OF GREENLAND
ZWALLY AND GIOVINETTO: MASS FLUX IN DRAINAGE SYSTEMS OF GREENLAND
ZWALLY AND GIOVINETTO: MASS FLUX IN DRAINAGE SYSTEMS OF GREENLAND
ZWALLY AND GIOVINETTO: MASS FLUX IN DRAINAGE SYSTEMS OF GREENLAND
ZWALLY AND GIOVINETTO: MASS FLUX IN DRAINAGE SYSTEMS OF GREENLAND
ZWALLY AND GIOVINETTO: MASS FLUX IN DRAINAGE SYSTEMS OF GREENLAND
ZWALLY AND GIOVINETTO: MASS FLUX IN DRAINAGE SYSTEMS OF GREENLAND
ZWALLY AND GIOVINETTO: MASS FLUX IN DRAINAGE SYSTEMS OF GREENLAND
ZWALLY AND GIOVINETTO: MASS FLUX IN DRAINAGE SYSTEMS OF GREENLAND
ZWALLY AND GIOVINETTO: MASS FLUX IN DRAINAGE SYSTEMS OF GREENLAND
ZWALLY AND GIOVINETTO: MASS FLUX IN DRAINAGE SYSTEMS OF GREENLAND
ZWALLY AND GIOVINETTO: MASS FLUX IN DRAINAGE SYSTEMS OF GREENLAND
ZWALLY AND GIOVINETTO: MASS FLUX IN DRAINAGE SYSTEMS OF GREENLAND
ZWALLY AND GIOVINETTO: MASS FLUX IN DRAINAGE SYSTEMS OF GREENLAND
ZWALLY AND GIOVINETTO: MASS FLUX IN DRAINAGE SYSTEMS OF GREENLAND
ZWALLY AND GIOVINETTO: MASS FLUX IN DRAINAGE SYSTEMS OF GREENLAND
ZWALLY AND GIOVINETTO: MASS FLUX IN DRAINAGE SYSTEMS OF GREENLAND
ZWALLY AND GIOVINETTO: MASS FLUX IN DRAINAGE SYSTEMS OF GREENLAND
ZWALLY AND GIOVINETTO: MASS FLUX IN DRAINAGE SYSTEMS OF GREENLAND
ZWALLY AND GIOVINETTO: MASS FLUX IN DRAINAGE SYSTEMS OF GREENLAND
ZWALLY AND GIOVINETTO: MASS FLUX IN DRAINAGE SYSTEMS OF GREENLAND
ZWALLY AND GIOVINETTO: MASS FLUX IN DRAINAGE SYSTEMS OF GREENLAND
ZWALLY AND GIOVINETTO: MASS FLUX IN DRAINAGE SYSTEMS OF GREENLAND
ZWALLY AND GIOVINETTO: MASS FLUX IN DRAINAGE SYSTEMS OF GREENLAND
ZWALLY AND GIOVINETTO: MASS FLUX IN DRAINAGE SYSTEMS OF GREENLAND
ZWALLY AND GIOVINETTO: MASS FLUX IN DRAINAGE SYSTEMS OF GREENLAND
ZWALLY AND GIOVINETTO: MASS FLUX IN DRAINAGE SYSTEMS OF GREENLAND

Table 1. Distribution of Accumulation by Diagenetic Facies Zonation (50 km Grid Database)

Physiographic Entity	Grid Point N	Area		Nominal Accumulation				Adjusted Accumulation	
		Nominal 10^6 km^2	Adjusted 10^6 km^2	Mean kg m^{-2} a^{-1}	s.d. kg m^{-2} a^{-1}	Min kg m^{-2} a^{-1}	Max kg m^{-2} a^{-1}	Mean kg m^{-2} a^{-1}	Bulk Gt a^{-1}
Based on Generalized Equilibrium Line									
Dry snow[a]	443	1.1075	1.1099	242	114	92	845	241	267
Lower percolation facies[b]	177	0.4425	0.4316	325	222	21	1500	321	139
Zone of net accumulation	620	1.5500	1.5415	266	158	21	1500	263	405
Zone of net ablation	62	0.1550	0.1497	-1267	986	-5000	0	-1259	-188
Conterminous ice sheet	682	1.7050	1.6913	127	552	-5000	1500	128	216
Based on Model Equilibrium Line									
Dry snow[a]	442	1.1050	1.1074	242	115	92	845	241	267
Lower percolation facies[b]	155	0.3875	0.3766	355	220	26	1500	341	132
Zone of net accumulation	597	1.4925	1.4840	272	157	26	1500	267	399
Zone of net ablation	85	0.2125	0.2073	-1123	910	-5000	0	-1086	-231
Conterminous ice sheet	682	1.7050	1.6913	98	580	-5000	1500	99	168

[a]Includes the zone of upper percolation facies.

[b]Includes zones of wetted facies and superimposed ice.

Table 2. Distribution of Accumulation by Drainage System (Model Equilibrium Line, 50 km Grid Database)

Drainage System		Zone of Net Ablation						Zone of Net Accumulation								
					Nominal Ablation	Adjusted Ablation					Nominal Accumulation				Adjusted Accumulation	
	Grid Point	Grid Point	Adjusted Area		Mean	Mean	Bulk	Grid Point	Adjusted Area		Mean	s.d.	Min	Max	Mean	Bulk
Designation	*N*	*N*	10^6 km^2	%	kg m^{-2} a^{-1}	kg m^{-2} a^{-1}	Gt a^{-1}	*N*	10^6 km^2	%	kg m^{-2} a^{-1}	kg m^{-2} a^{-1}	kg m^{-2} a^{-1}	kg m^{-2} a^{-1}	kg m^{-2} a^{-1}	Gt a^{-1}
1	100	4	0.0102	4.0	-900	-918	-9.2	96	0.2457	96.0	170	57	26	458	174	41.8
2	135	9	0.0229	6.7	-1111	-1131	-25.5	126	0.3193	93.3	132	37	30	293	134	42.3
3	99	11	0.0270	11.1	-727	-717	-19.7	88	0.2172	88.9	283	92	57	488	279	61.3
3m	93	8	0.0197	8.6	-691	-682	-13.7	85	0.2099	91.4	283	92	57	488	279	59.3
4	71	16	0.0373	22.2	-1897	-1759	-70.4	55	0.1310	77.8	537	249	184	1500	509	70.0
5	178	33	0.0796	18.5	-1011	-977	-80.6	145	0.3516	81.5	343	107	100	660	333	120.6
6	99	12	0.0302	12.1	-842	-848	-25.4	87	0.2190	87.9	287	68	180	575	289	62.9
1-6	682	85	0.2073	12.3	-1123	-1086	-230.7	597	1.4840	87.7	272	157	26	1500	267	398.9
1-6m	676	82	0.1999	11.9	-1134	-1096	-224.7	594	1.4767	88.1	272	157	26	1500	267	396.9

Table 3. Balance Mass Flux at the Cross Section Aligned With the Model Equilibrium Line and Related Estimates (50 km Grid Database)

			Equilibrium Line Cross Section							Drainage System			
DrSy Desig.	Gr Pt. *N*	Bulk Acc. Gt a^{-1}	Sampled %	Length km	Ice Thick. km	Area km^2	Flux Gt km^{-2} a^{-1}	Discharge Gt km^{-1} a^{-1}	Ice Movement km a^{-1}	Area 10^6 km^2	Ice Thickness km	Ice Mass Tt	Total Mass Exchange ka
1	96	41.8	69	2005	0.229	459.1	0.0910	0.0208	0.100	0.2457	1.609	355.798	8.5
2	126	42.3	76	934	0.497	464.2	0.0911	0.0453	0.100	0.3193	2.072	595.431	14.1
3	88	61.3	42	2418	0.349	843.9	0.0726	0.0254	0.080	0.2172	1.424	278.364	4.5
3m	85	59.3	48	1873	0.349	653.7	0.0907	0.0317	0.100	0.2099	1.474	278.453	4.7
4	55	70.0	75	1403	0.455	638.4	0.1097	0.0499	0.121	0.1310	1.590	187.461	2.7
5	145	120.6	98	1373	0.744	1021.5	0.1181	0.0878	0.130	0.3516	2.075	656.613	5.4
6	87	62.9	84	831	0.646	536.8	0.1172	0.0757	0.129	0.2190	2.105	414.895	6.6
1-6	597	398.9	69	8964	0.442	3963.9	0.0956	0.0435	0.105	1.4840	1.863	2488.223	6.2
1-6m	594	396.9	72	8419	0.448	3773.2	0.1011	0.0468	0.111	1.4767	1.873	2489.273	6.3

Table 4. Summary of Surface Balance and Related Estimates (All Values in Gt a^{-1})

Source	Net Accumulation	Net Ablation	Gross Accumulation	Gross Ablation	Surface Balance	Difference From This Study
This study[a,b]	399	231	—	—	168	—
F. Jung-Rothenhäusler et al., (unpub. data, 2000)	—	—	510	NA	NA	—
Janssens and Huybrechts [2000]	—	—	542	281	261	93
Zwally and Giovinetto [2000][a,c]	405	188	—	—	217	49
Ohmura et al. [1999]	—	—	516	347	169	1
Reeh et al. [1999]	—	—	547	276	271	103
van de Wal [1996]	—	—	539	316	223	55
Giovinetto and Zwally [1995][a,c]	431	232[d]	—	—	199	31
Robasky and Bromwich [1994]	—	—	545	NA	NA	—
Ohmura and Reeh [1991]	—	—	535	NA	NA	—
Huybrechts et al. [1991]	—	—	539	256	283	115
Reeh [1985]	—	—	487	169	318	150
Weidick [1984]	—	—	500	295	205	37
Radok et al. [1982] Inner Equilibrium Line	486	139	—	—	347	179
Radok et al. [1982] Outer Equilibrium Line	576	69	—	—	507	339

[a]Estimate for the area of the conterminous ice sheet; others may include the area of separate ice caps.

[b]Estimate based on the model equilibrium line.

[c]Estimate based on the generalized equilibrium line.

[d]Ablation estimate based on middle range of three estimates [*Ambach*, 1982; *Weidick*, 1984; *Reeh*, 1985].

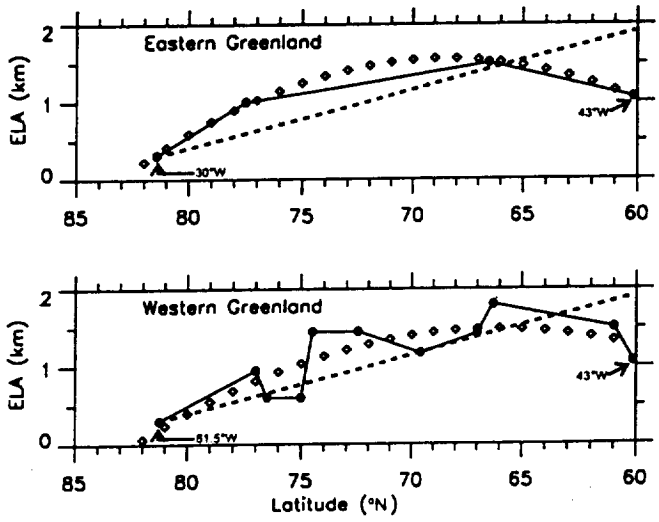
Eastern Greenland
ELA (km)
2
1
0
43°W
30°W
85
80
75
70
65
60
Western Greenland
ELA (km)
2
1
0
43°W
61.5°W
85
80
75
70
65
60
Latitude (°N)

Fig 1

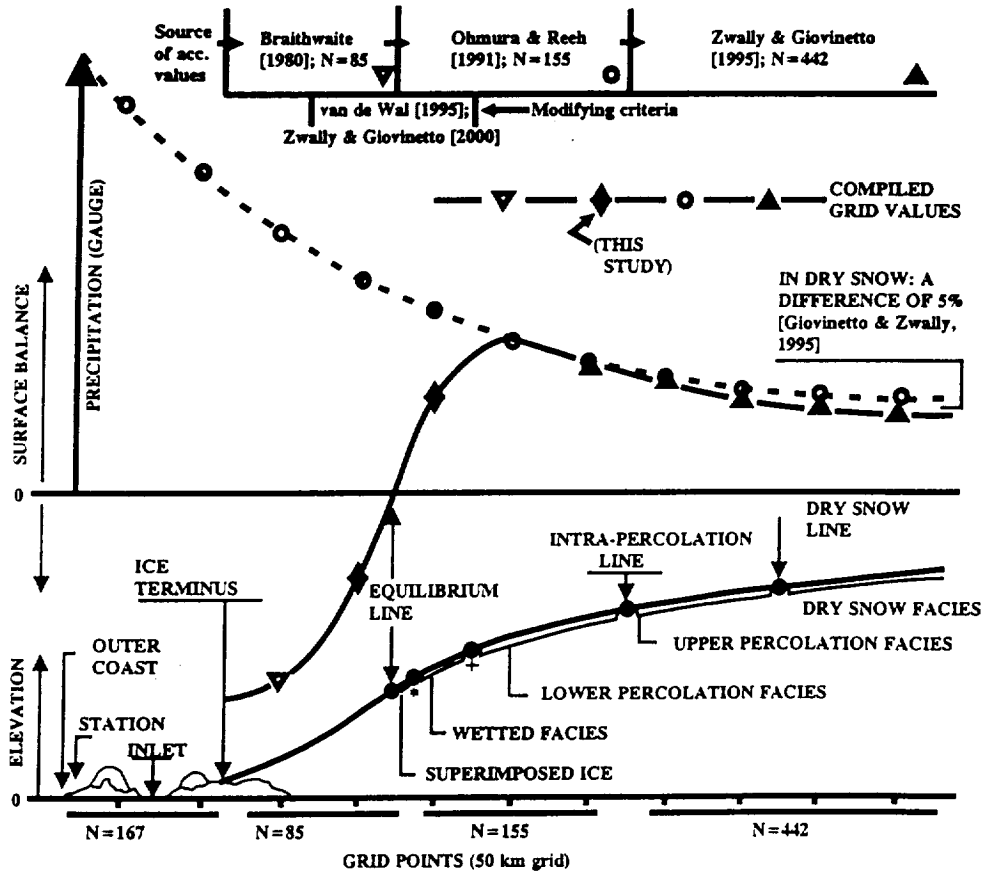

* FIRN LINE (SNOW LINE); + SATURATION LINE [Benson, 1962], WET-SNOW LINE [Benson, 1994].

FIG. 2

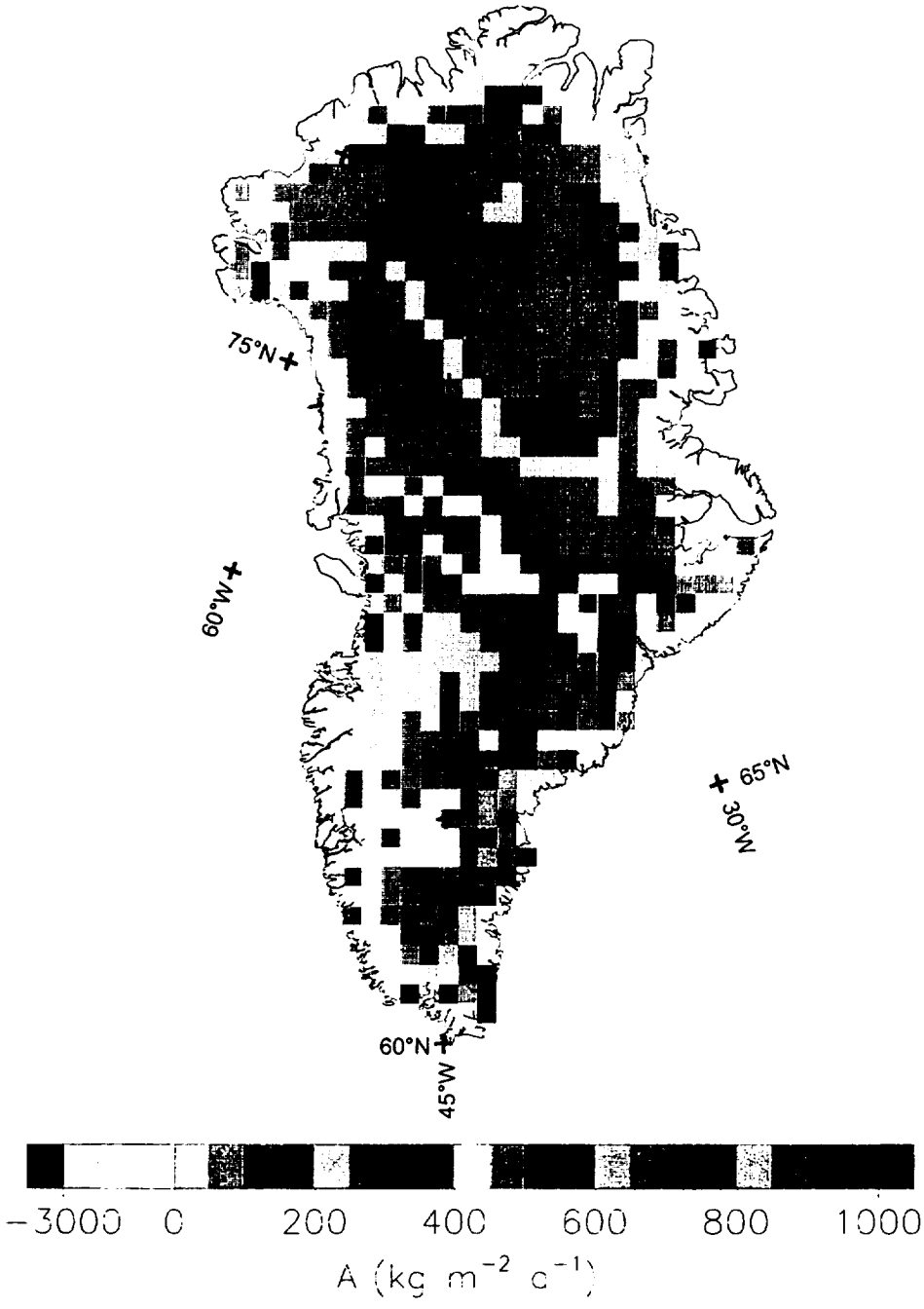

Plate 1

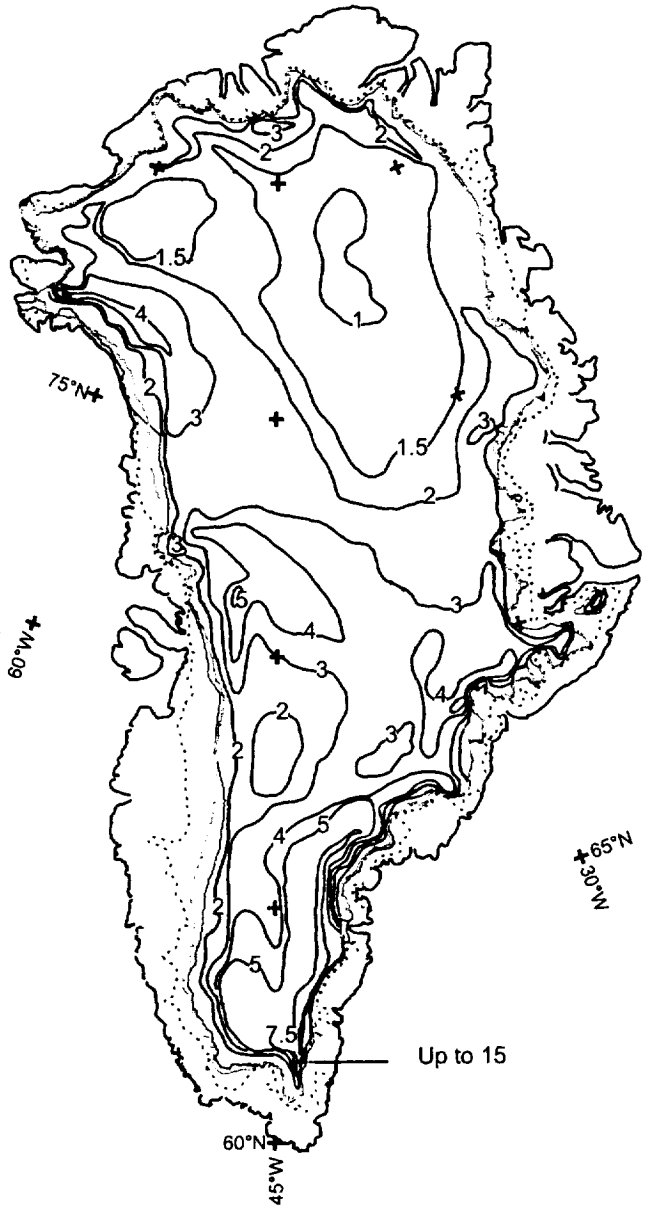

Plate 2

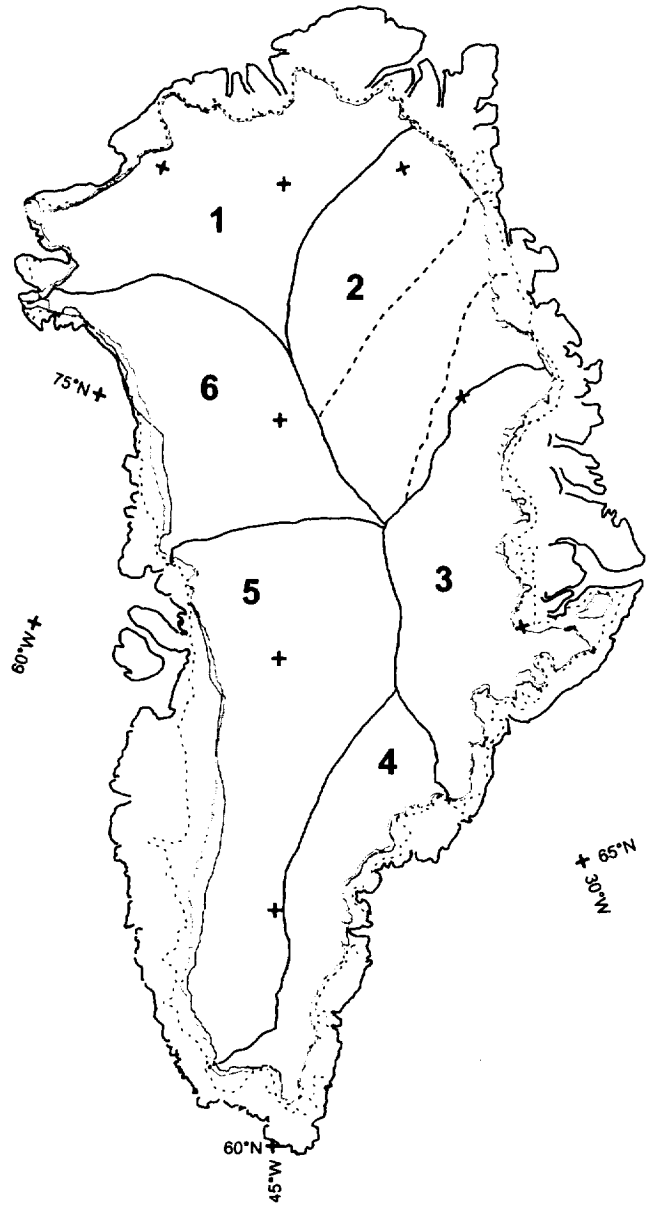

Plate 3

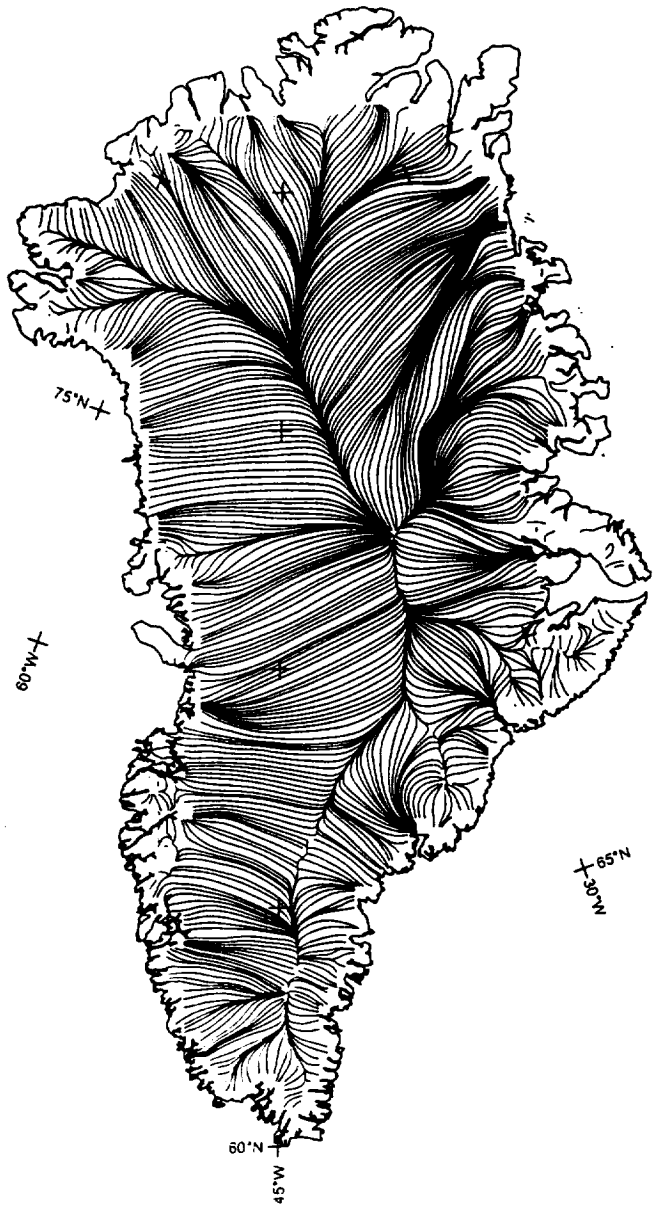

FIG. 3